

Intelligent Reflecting Surface Empowered UAV SWIPT Networks

Zhendong Li, Wen Chen, *Senior Member, IEEE*, Huanqing Cao, Hongying Tang, Kunlun Wang, *Member, IEEE*, and Jun Li, *Senior Member, IEEE*

Abstract—Aiming at the limited battery capacity of a large number of widely deployed low-power smart devices in the Internet-of-things (IoT), this paper proposes a novel intelligent reflecting surface (IRS) empowered unmanned aerial vehicle (UAV) simultaneous wireless information and power transfer (SWIPT) network framework, in which IRS is used to reconstruct the wireless channel to enhance the energy transmission efficiency and coverage of the UAV SWIPT networks. In this paper, we formulate an achievable sum-rate maximization problem by jointly optimizing UAV trajectory, UAV transmission power allocation, power splitting (PS) ratio and IRS reflection coefficient under a non-linear energy harvesting model. Due to the coupling of optimization variables, this problem is a complex non-convex optimization problem, and it is challenging to solve it directly. We first transform the problem, and then apply the alternating optimization (AO) algorithm framework to divide the transformed problem into four blocks to solve it. Specifically, by applying successive convex approximation (SCA) and difference-convex (DC) programming, UAV trajectory, UAV transmission power allocation, PS ratio and IRS reflection coefficient are alternately optimized when the other three are given until convergence is achieved. Numerical simulation results verify the effectiveness of our proposed algorithm compared to other algorithms.

Index Terms—IRS, UAV, simultaneous wireless information and power transfer, alternating optimization, successive convex approximation, difference-convex programming.

I. INTRODUCTION

NOWADAYS, with the vigorous development of the Internet-of-things (IoT), the number of smart devices is growing rapidly [1]–[3]. These smart devices used to collect and send information have the characteristics of low power consumption and limited battery capacity. It is an effective way to replace the battery or charge the battery [3]. However, if the smart devices in IoT are large-scale, such operations are time-consuming and laborious.

Z. Li, W. Chen and H. Cao are with the Department of Electronic Engineering, Shanghai Jiao Tong University, Shanghai 200240, China (e-mail: lizhendong@sjtu.edu.cn; wenchen@sjtu.edu.cn; caohuanqing@sjtu.edu.cn).

H. Tang is with the Science and Technology on Microsystem Laboratory, Shanghai Institute of Microsystem and Information Technology, Chinese Academy of Sciences, Shanghai 200050, China (e-mail: tanghy@mail.sim.ac.cn).

K. Wang is with the School of Information Science and Technology, ShanghaiTech University, Shanghai 201210, China, and also with the School of Communication and Electronic Engineering, East China Normal University, Shanghai 200241, China (e-mail: wangk12@shanghaitech.edu.cn).

J. Li is with the School of Electronic and Optical Engineering, Nanjing University of Science Technology, Nanjing 210094, China (email: jun.li@njust.edu.cn).

(Corresponding author: Wen Chen.)

Wireless power transfer (WPT) is a promising technology that can solve the above-mentioned challenges. This technology has the advantages of flexibility, easy deployment, and no contact, so it has received extensive attention from industry and academia [4]–[8]. For devices with low power consumption and limited battery capacity in IoT, wireless charging devices can dynamically join or leave the network, which is more effective. Simultaneous wireless information and power transfer (SWIPT) technology is a scheme in WPT [9]. Through SWIPT, users can get information and energy transmission at the same time, which brings great convenience to the deployment of IoT devices. As one of the design schemes of SWIPT practical receivers, the power splitting (PS) scheme divides the signal received by the receiver into two different power streams, one part is used to decode information, and the other part is used to harvest energy [9]. However, smart devices are usually widely distributed to collect data in IoT. Therefore, it is challenging for these smart devices to harvest energy from a fixed energy station. Although this problem can be solved by increasing the number of power stations in the target area, the deployment cost of these power stations may be very high.

In recent years, unmanned aerial vehicles (UAVs) have been widely used in different fields. Compared with traditional fixed access points (APs), UAVs equipped with APs have the advantages of dynamic mobility, flexibility and ease of deployment, and low cost [10]–[16]. UAVs equipped with wireless energy stations can better solve the battery capacity limitation problem of widely deployed smart devices in IoT. Therefore, the research on UAV-assisted WPT networks has also attracted the attention of the academic community [17]–[22]. Sun *et al.* investigated physical layer security enhancement methods for millimeter-wave (mmWave) UAV SWIPT networks [18]. Wang *et al.* proposed UAV-assisted NOMA to achieve SWIPT and guarantee the secure transmission for ground passive receivers (PRs), in which the nonlinear energy harvesting model is applied [19]. Chen *et al.* considered UAV-enabled WPCN, where UAV coordinates the wireless energy/information transmissions to/from a set of nodes and aims to minimize the transmission completion time (TCT) of collecting a given number of bits per node [21]. However, for UAV-assisted WPT networks, due to distance-related propagation loss, the energy transmission efficiency will decrease as the distance increases, which greatly limits the coverage of UAV-assisted SWIPT. If the wireless channel can be reconstructed and the channel gain can be increased, the coverage of the networks can be greatly

improved, which greatly stimulates the use of new network paradigms to improve the performance of the UAV-assisted WPT networks.

Intelligent reflecting surface (IRS), also called reconfigurable intelligent surface (RIS), as a revolutionary technology, has been studied extensively by industry and academia [23]–[26], which can reconstruct the wireless channel from the transmitter to the receiver by adjusting the amplitude and phase of the incident signal, thereby improving network performance. In detail, an IRS is an array composed of a large number of low-cost passive reflecting elements, which can be easily deployed on indoor walls or buildings. Since the IRS is a passive device, it only passively reflects the incident signal without signal processing, so it will not introduce unnecessary noise compared with the relay [27]. Meanwhile, compared with MIMO technology, the required hardware cost and power consumption are much lower [28]. These have greatly promoted the application of IRS in the next generation communication networks.

In view of the advantages of IRS, the energy transmission efficiency and coverage of the IRS-assisted UAV WPT network can be greatly improved. At present, research on the IRS-assisted UAV communication network has been carried out [29]–[33]. Taniya *et al.* proposed a theoretical framework to analyze the performance of an UAV-IRS networks where the IRS provides an additional degree of freedom combined with the flexible deployment of full-duplex UAV to enhance communication between ground nodes [29]. Mu *et al.* investigated IRS enhanced UAV non-orthogonal multiple access (NOMA) networks, where the three-dimensional (3D) placement and transmit power of UAVs, the IRS reflection matrix, and the NOMA decoding orders among users are jointly optimized for maximization of the sum-rate [32]. Li *et al.* maximized the average worst-case secrecy rate by the robust joint design of the UAV's trajectory, RIS passive beamforming, and transmit power of the legitimate transmitters in UAV secure communication system [33]. However, as far as we know, there is no research on IRS-assisted dynamic UAV WPT network. In this paper, we consider the IRS-assisted dynamic UAV SWIPT network, in which dynamic UAV can greatly release its potential. We maximize the achievable sum-rate by jointly optimizing UAV trajectory, UAV transmission power allocation, PS ratio and IRS reflection coefficient. Due to the high coupling of optimization variables, the concavity and convexity of the objective function and some constraints cannot be determined, so it is challenging to solve this problem directly. Therefore, we need to design an effective algorithm for IRS-assisted UAV-enabled SWIPT networks.

Based on the above background, the main contributions of this paper can be summarized as follows:

- Facing the limited battery capacity of smart devices with widely distributed and low power consumption in IoT networks, we proposed an IRS empowered UAV SWIPT framework. Smart devices use PS, which allows them to harvest energy while receiving information. Meanwhile, we formulate an achievable sum-rate maximization problem, which jointly optimizes UAV trajectory, UAV transmission power allocation, PS ratio and IRS reflection

coefficient. Since this problem is a complex non-convex optimization problem, it is challenging to solve it directly.

- In order to solve the above sum-rate maximization problem, we first transform the problem, and then use the alternating optimization (AO) framework to divide the transformed problem into four blocks. Specifically, first, given UAV transmit power allocation, PS ratio, and IRS reflection coefficient, UAV trajectory can be obtained by applying successive convex approximation (SCA). Given the UAV trajectory, transmit power allocation, and IRS reflection coefficient, the PS ratio problem is a linear programming (LP) problem, and its solution is easy to obtain. Similarly, UAV transmit power allocation and IRS phase shift coefficients can also be obtained separately by using SCA and difference-convex (DC) programming when the other three blocks are given. Finally, the four blocks are alternately optimized until convergence is achieved.
- Through numerical simulation, we verify the effectiveness of the proposed optimization algorithm of UAV trajectory, UAV transmission power allocation, PS ratio and IRS reflection coefficient compared with the algorithms, i.e., it can improve the achievable sum-rate of the system. For the UAV SWIPT network assisted by IRS, the sum-rate is significantly higher than that of the network without IRS assistance. Meanwhile, the more reflective elements of the IRS, the higher the achievable sum-rate.

The remainder of this paper is organized as follows. Section II elaborates the system model and optimization problem formulation for the IRS empowered UAV SWIPT networks. Section III presents the proposed optimization algorithm for the formulated optimization problem. In Section IV, numerical results demonstrate that our algorithm has good convergence and effectiveness. Finally, the conclusion is given in Section V.

Notations: Scalars are denoted by lower-case letters, while vectors and matrices are represented by bold lower-case letters and bold upper-case letters, respectively. $|x|$ denotes the absolute value of a complex-valued scalar x , and $\|\mathbf{x}\|$ denotes the Euclidean norm of a complex-valued vector \mathbf{x} . $\text{diag}(\mathbf{x})$ denotes a diagonal matrix whose diagonal elements are the corresponding elements in vector \mathbf{x} . For a square matrix \mathbf{X} , $\text{tr}(\mathbf{X})$, $\text{rank}(\mathbf{X})$, \mathbf{X}^H and $\mathbf{X}_{m,n}$ denote its trace, rank, conjugate transpose and m, n -th entry, respectively, while $\mathbf{X} \succeq 0$ represents that \mathbf{X} is a positive semidefinite matrix. $\mathbb{C}^{M \times N}$ denotes the space of $M \times N$ complex matrices. j denotes the imaginary unit, i.e., $j^2 = -1$. $\mathbb{E}\{\cdot\}$ represents the expectation of random variables. Finally, the distribution of a circularly symmetric complex Gaussian (CSCG) random vector with mean μ and covariance matrix \mathbf{C} is denoted by $\mathcal{CN}(\mu, \mathbf{C})$, and \sim stands for ‘distributed as’.

II. SYSTEM MODEL AND PROBLEM FORMULATION

A. System model

In this paper, we consider an IRS empowered downlink UAV SWIPT network in IoT consisting of a rotary-wing UAV with a single omni-directional antenna, an IRS and K single

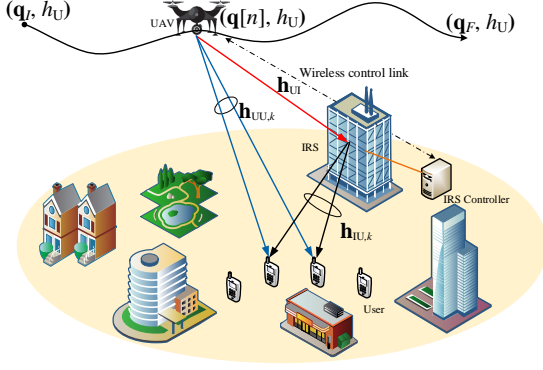


Fig. 1. IRS empowered UAV SWIPT networks.

antenna users (i.e., smart devices). As shown as in Fig. 1, the UAV simultaneously sends signals to ground users. The IRS can be deployed on a building to assist the SWIPT networks from the UAV to users, which is equipped with a uniform linear array (ULA) of M reflecting elements¹. Meanwhile, the IRS is also equipped with a smart controller, which coordinates the UAV and IRS for both channel acquisition and information and power transmission. We assume that all channels in this paper are quasi-static flat-fading and the channel state information (CSI) of all channels is perfectly known at the UAV.

Without loss of generality, we consider a 3D Cartesian coordinate system, where the k -th single-antenna user's coordinate is $\mathbf{w}_k = [x_k, y_k, 0]^T$. The UAV flies at a fixed altitude h_u , which is the minimum altitude to avoid any collision with building. We consider a finite time period T to guarantee the efficiency of simultaneous information and power transmission. For simplicity, the time period T is divided into N time slots, indexed by $n = 1, \dots, N$. Each time slot $\delta = \frac{T}{N}$ is selected to be small enough to ensure that the UAV position is approximately unchanged when flying at the maximum speed V_{\max} . Hence, the 3D trajectory of UAV can be approximated by $\mathbf{q}[n] = [x[n], y[n], h_u]^T, n = 1, \dots, N$. We consider the initial and final position of the UAV can be denoted by \mathbf{q}_I and \mathbf{q}_F , respectively. The trajectory of UAV should satisfy the following constraints

$$\mathbf{q}_I = \mathbf{q}[1], \quad (1)$$

$$\mathbf{q}_F = \mathbf{q}[N], \quad (2)$$

$$\|\mathbf{q}[n+1] - \mathbf{q}[n]\|^2 \leq (V_{\max}\delta)^2, n = 1, \dots, N-1. \quad (3)$$

Let $p_k[n]$ denote the transmission power allocated to the k -th user by the UAV in the n -th time slot. Without loss of generality, it should satisfy the following constraints

$$p_k[n] \geq 0, \forall k, n, \quad (4)$$

¹It is worth noting that the algorithm proposed in this paper can be extended to the IRS equipped with a uniform planar array (UPA) by considering the corresponding antenna array response.

$$\sum_{k=1}^K p_k[n] \leq P_{\max}, \forall n, \quad (5)$$

where P_{\max} denotes the maximum transmission power of the UAV.

For the IRS with M reflecting elements, each element reflects the received signal from the UAV with an adjustable amplitude and phase shift. Let $\boldsymbol{\theta}[n] = [\theta_1[n], \dots, \theta_M[n]] \in \mathbb{C}^{1 \times M}, \forall n$, and we model the IRS reflection matrix by using $\boldsymbol{\Theta}[n] = \text{diag}(\beta_1[n] e^{j\theta_1[n]}, \dots, \beta_M[n] e^{j\theta_M[n]}) \in \mathbb{C}^{M \times M}$, where $\theta_m[n] \in [0, 2\pi), \forall m, n$ and $\beta_m[n] \in [0, 1], \forall m, n$ denote the phase shift and amplitude reflection coefficient of the m -th IRS element, respectively. For simplicity, we set $\beta_m[n] = 1$ to achieve the maximum reflecting power gain. In the n -th time slot, the phase shift of the m -th element should satisfy the following constraint

$$0 \leq \theta_m[n] < 2\pi, \forall m, n. \quad (6)$$

Furthermore, the first element of the IRS is regarded as the reference point whose 3D coordinate can be denoted by $\mathbf{w}_r = [x_r, y_r, h_r]^T$, respectively. Hence, the distance between the IRS and the UAV or the ground users can be approximated by that between the reference point and the corresponding node. The channel gain from the UAV to the IRS, from the UAV to the k -th ground user, and from the IRS to the k -th ground user can be denoted by $\mathbf{h}_{UI} \in \mathbb{C}^{M \times 1}, h_{UU,k} \in \mathbb{C}$, and $\mathbf{h}_{IU,k} \in \mathbb{C}^{M \times 1}$, respectively.

Since the UAV usually flies at a high altitude and the IRS is commonly placed on the building, the link from the UAV to the IRS (UI-link) is modeled to be a line-of-sight (LoS) channel. The link from the UAV to the k -th ground user (UU-link) is assumed to be Rayleigh fading channel since there exist extensive scatters in the urban scenario. Besides, the link from the IRS to the k -th ground user (IU-link) can be modeled by a Rician fading channel. In this paper, we apply ULA at the IRS. Therefore, the LoS component can be expressed by the responses of the ULA. The array response of M -element ULA of the IRS in the n -th time slot can be given by

$$\mathbf{h}[n] = \left[1, e^{-j2\pi \frac{d}{\lambda} \cos \phi[n]}, \dots, e^{-j2\pi \frac{d}{\lambda} (M-1) \cos \phi[n]} \right]^T, \forall n, \quad (7)$$

where $\phi[n]$ is angle of arrival (AoA) of a signal at the IRS in the n -th time slot, $\cos \phi[n] = \frac{x_r - x[n]}{\|\mathbf{q}[n] - \mathbf{w}_r\|}$, λ is the carrier wavelength, and d represents the array interval. Therefore, the channel gain of the UI-link in the n -th time slot can be denoted by

$$\mathbf{h}_{UI}[n] = \sqrt{\frac{\beta_0}{\|\mathbf{q}[n] - \mathbf{w}_r\|^2}} \mathbf{h}[n], \forall n, \quad (8)$$

where β_0 is the path loss when the reference distance is 1m.

The channel gain of the UU link in the n -th time slot can be expressed by

$$h_{UU,k}[n] = \sqrt{\frac{\beta_0}{\|\mathbf{q}[n] - \mathbf{w}_k\|^\alpha}} \tilde{h}, \forall k, n, \quad (9)$$

where α is the corresponding path loss exponent related to the UU link. $\tilde{h} \in \mathbb{C}$ represents the random scattering com-

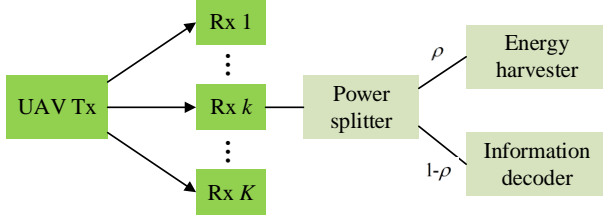


Fig. 2. PS receiver architecture.

ponent modeled by a zero-mean and unit-variance circularly symmetric complex Gaussian (CSCG) random variable.

The channel gain of the IU link can be denoted by

$$\mathbf{h}_{\text{IU},k} = \sqrt{\frac{\beta_0}{\|\mathbf{w}_r - \mathbf{w}_k\|^\gamma}} \left(\sqrt{\frac{\kappa}{1+\kappa}} \mathbf{h}_{\text{IU},k}^{\text{LoS}} + \sqrt{\frac{1}{1+\kappa}} \mathbf{h}_{\text{IU},k}^{\text{NLoS}} \right), \forall k, \quad (10)$$

where γ is the corresponding path loss exponent related to the IU link and κ is the Rician factor. The LoS component $\mathbf{h}_{\text{IU},k}^{\text{LoS}} \in \mathbb{C}^{M \times 1}$ can be denoted by

$$\mathbf{h}_{\text{IU},k}^{\text{LoS}} = \left[1, e^{-j2\pi \frac{d}{\lambda} \cos \varphi_k}, \dots, e^{-j2\pi \frac{d}{\lambda} (M-1) \cos \varphi_k} \right]^T, \forall k, \quad (11)$$

where φ_k is the angle of departure (AoD) of a signal from the IRS to the k -th ground user, $\cos \varphi_k = \frac{x_k - x_r}{\|\mathbf{w}_r - \mathbf{w}_k\|}$. And the NLoS component $\mathbf{h}_{\text{IU},k}^{\text{NLoS}} \in \mathbb{C}^{M \times 1}$ is with the variables independently drawn from the CSCG distribution with zero mean and unit variance. Therefore, the combined channel gain from UAV to the k -th user in the n -th time slot can be expressed as

$$H_k[n] = |h_{\text{UU},k}[n] + \mathbf{h}_{\text{IU},k}^H \Theta[n] \mathbf{h}_{\text{UI}}[n]|^2, \forall k, n. \quad (12)$$

The signal received by the k -th user in the n -th slot can be expressed as

$$y_k[n] = (h_{\text{UU},k}[n] + \mathbf{h}_{\text{IU},k}^H \Theta[n] \mathbf{h}_{\text{UI}}[n]) \sum_{k=1}^K \sqrt{p_k[n]} s_k[n], \forall k, n. \quad (13)$$

In this paper, we consider the power splitting (PS) receiver architecture at the ground users for information decoding and energy harvesting, which is actually one of the most widely used architectures in SWIPT networks. The architecture diagram is shown in the Fig. 2. Specifically, In the n -th time slot, the radio frequency (RF) signal received by the k -th ground user is split with a PS ratio $\rho_k[n]$, which should satisfy the following constraint

$$0 \leq \rho_k[n] \leq 1, \forall k, n, \quad (14)$$

which represents the PS ratio of each ground user in the n -th time slot should be between zero and one. The $\rho_k[n]$ portion of the received power is used by the k -th user for energy harvesting in the n -th time slot, and the $(1 - \rho_k[n])$ portion is used by the k -th user for decoding the information in the n -th time slot. Therefore, the signal to interference plus noise

ratio (SINR) of the k -th user for information decoding in the n -th slot can be expressed as

$$\text{SINR}_k[n] = \frac{(1 - \rho_k[n]) p_k[n] H_k[n]}{(1 - \rho_k[n]) \left(\sum_{i \neq k}^K p_i[n] H_k[n] + \sigma^2 \right)}, \forall k, n, \quad (15)$$

where σ^2 is the power of the additive white Gaussian noise (AWGN) at the k -th user. Therefore, the achievable rate of the k -th ground user in the n -th time can be expressed as

$$R_k[n] = \log_2(1 + \text{SINR}_k[n]), \forall k, n. \quad (16)$$

Therefore, the achievable sum-rate for the k -th user in the time period T can be expressed as

$$R_{\text{sum}} = \sum_{n=1}^N \sum_{k=1}^K R_k[n], \forall k. \quad (17)$$

In addition, the received power of the k -th user in the n -th time slot can be given

$$P_k[n] = \rho_k[n] \left(\sum_{i=1}^K p_i[n] H_k[n] \right), \forall k, n. \quad (18)$$

Furthermore, in order to accurately describe the harvested energy, this paper adopts the nonlinear energy harvested model based on the practical system, thus the harvested power of the k -th user in the n -th time can be given by

$$\Xi(P_k[n]) = \left(\frac{\xi_k}{X_k (1 + \exp(-a_k(P_k[n] - b_k)))} - Y_k \right), \forall k, \forall n, \quad (19)$$

where ξ_k denotes the maximum power that the k -th user can harvest, a_k and b_k are parameters related to specific circuit specifications, $X_k = \exp(a_k b_k) / (1 + \exp(a_k b_k))$ and $Y_k = \xi_k / \exp(a_k b_k)$ [34]. Then the harvested energy of the k -th user in the n -th time slot can be given

$$E_k[n] = \delta \Xi(P_k[n]), \forall k, n, \quad (20)$$

The average harvested energy for the k -th user in the time period T can be expressed as

$$E_k = \frac{1}{N} \sum_{n=1}^N E_k[n], \forall k. \quad (21)$$

In order to meet the energy constraint of the k -th ground user, E_k needs to meet the following constraint

$$E_k \geq \chi_k, \forall k, \quad (22)$$

where χ_k is the energy constraint of the k -th ground user. It can be seen from Eq. (16) and (22) that there is a tradeoff between the achievable rate and harvested energy for the k -th user in the n -th time slot.

B. Problem formulation

In this paper, we maximize the achievable sum-rate for all users in the IRS empowered UAV SWIPT networks by jointly optimizing UAV trajectory $\mathbf{Q} = \{\mathbf{q}[n], \forall n\}$, UAV transmission power allocation $\mathbf{p} = \{p_k[n], \forall k, n\}$, PS ratio

$\boldsymbol{\rho} = \{\rho_k[n], \forall k, n\}$ and IRS reflection coefficient $\boldsymbol{\theta} = \{\theta_m[n], \forall m, n\}$. The optimization problem can be formulated as follows

$$\mathcal{P}1: \quad \max_{\mathbf{Q}, \mathbf{p}, \boldsymbol{\rho}, \boldsymbol{\theta}} R_{\text{sum}}, \quad (23a)$$

$$s.t. \quad \mathbf{q}_I = \mathbf{q}[1], \quad (23b)$$

$$\mathbf{q}_F = \mathbf{q}[N], \quad (23c)$$

$$\|\mathbf{q}[n+1] - \mathbf{q}[n]\|^2 \leq (V_{\max}\delta)^2, n = 1, \dots, N-1, \quad (23d)$$

$$p_k[n] \geq 0, \forall k, n, \quad (23e)$$

$$\sum_{k=1}^K p_k[n] \leq P_{\max}, \forall n, \quad (23f)$$

$$0 \leq \theta_m[n] \leq 2\pi, \forall m, n, \quad (23g)$$

$$0 \leq \rho_k[n] \leq 1, \forall k, n, \quad (23h)$$

$$E_k \geq \chi_k, \forall k, \quad (23i)$$

where (23b), (23c) and (23d) are UAV trajectory constraint, (23e) and (23f) are UAV transmission power allocation constraint, (23g) is IRS reflection coefficients constraint, (23h) is the PS ratio constraint in SWIPT, and (23i) is the energy harvested threshold of the k -th user. The joint optimization problem $\mathcal{P}1$ is a nonconvex optimization problem since the objective function and the constraint (23i) are not jointly concave with respect to (w.r.t.) the whole optimization variables. Hence, it is challenging to solve the problem $\mathcal{P}1$ directly.

III. PROBLEM SOLUTION

Since the objective function of problem $\mathcal{P}1$ contains random variables, we take expectation on it to transform the problem. Then, for the transformed problem, we use AO algorithm to solve it. More specifically, we divide the optimization problem into four blocks, i.e., \mathbf{Q} , \mathbf{p} , $\boldsymbol{\rho}$ and $\boldsymbol{\theta}$. For given UAV transmission power allocation \mathbf{p} , user PS ratio $\boldsymbol{\rho}$ and IRS reflection coefficient $\boldsymbol{\theta}$, the trajectory of UAV \mathbf{Q} can be obtained. Next, for given the UAV trajectory \mathbf{Q} , UAV transmission power allocation \mathbf{p} and user PS ratio $\boldsymbol{\rho}$, we can get the IRS reflection coefficient $\boldsymbol{\theta}$. Then, UAV transmission power allocation \mathbf{p} can be solved when the UAV trajectory \mathbf{Q} , IRS reflection coefficient $\boldsymbol{\theta}$ and user PS ratio $\boldsymbol{\rho}$ are fixed. Finally, We can also get user PS ratio $\boldsymbol{\rho}$ by fixing the UAV trajectory \mathbf{Q} , IRS reflection coefficient $\boldsymbol{\theta}$ and UAV transmission power allocation \mathbf{p} . When solving the above problems, we adopt SCA and DC programming.

A. Optimization problem transformation

Since the objective function $R_k[n]$ of the optimization problem $\mathcal{P}1$ contains random variables, we take the expectation $\mathbb{E}\{R_k[n]\}$ to analyze it. Since the probability distribution of $R_k[n]$ is difficult to obtain, it is not easy to find a closed-form solution of $\mathbb{E}\{R_k[n]\}$. Thus, we use the following **Lemma 1** to approximate $\mathbb{E}\{R_k[n]\}$.

Lemma 1: If X is a positive random variable, for any $\psi > 0$, $\varphi > 0$ and $\phi > 0$, the following approximation result holds

$$\mathbb{E}\left\{\log_2\left(1 + \frac{\psi}{\varphi + \frac{\phi}{X}}\right)\right\} \approx \mathbb{E}\left\{\log_2\left(1 + \frac{\psi}{\varphi + \frac{\phi}{\mathbb{E}\{X}\}}\right)\right\}. \quad (24)$$

Proof: The proof of **Lemma 1** is similar to Theorem 1 in [35], which is omitted here.

We first take an expectation of $H_k[n]$ as follows

$$\begin{aligned} \mathbb{E}\{H_k[n]\} &= \mathbb{E}\left\{\left|h_{\text{UU},k}[n] + \left(\widetilde{\mathbf{h}}_{\text{IU},k}^H + \widetilde{\mathbf{h}}_{\text{IU},k}^H\right) \boldsymbol{\Theta}[n] \mathbf{h}_{\text{UI}}[n]\right|^2\right\} \\ &= \mathbb{E}\left\{\left|h_{\text{UU},k}[n]\right|^2\right\} + \mathbb{E}\left\{\left|\widetilde{\mathbf{h}}_{\text{IU},k}^H \boldsymbol{\Theta}[n] \mathbf{h}_{\text{UI}}[n]\right|^2\right\} \\ &+ \mathbb{E}\left\{\left|\widetilde{\mathbf{h}}_{\text{IU},k}^H \boldsymbol{\Theta}[n] \mathbf{h}_{\text{UI}}[n]\right|^2\right\} = \frac{\beta_0}{\|\mathbf{q}[n] - \mathbf{w}_k\|^\alpha} \\ &+ \frac{N\beta_0(\beta_0 - \vartheta)}{\|\mathbf{q}[n] - \mathbf{w}_r\|^2 \|\mathbf{w}_r - \mathbf{w}_k\|^\gamma} + \left|\widetilde{\mathbf{h}}_{\text{IU},k}^H \boldsymbol{\Theta}[n] \mathbf{h}_{\text{UI}}[n]\right|^2 \triangleq \xi_k[n], \end{aligned} \quad (25)$$

where $\widetilde{\mathbf{h}}_{\text{IU},k}^H = \sqrt{\frac{\vartheta}{\|\mathbf{w}_r - \mathbf{w}_k\|^\gamma}} \mathbf{h}_{\text{IU},k}^{\text{LoS}}$, $\widetilde{\mathbf{h}}_{\text{IU},k}^H = \sqrt{\frac{\beta_0 - \vartheta}{\|\mathbf{w}_r - \mathbf{w}_k\|^\gamma}} \mathbf{h}_{\text{IU},k}^{\text{NLoS}}$ and $\vartheta = \frac{\beta_0 \kappa}{1 + \kappa}$. Thus,

$$\begin{aligned} \mathbb{E}\{R_k[n]\} &\approx \mathbb{E}\left\{\log_2\left(1 + \frac{(1 - \rho_k[n]) p_k[n]}{(1 - \rho_k[n]) \left(\sum_{i \neq k}^K p_i[n] + \frac{\sigma^2}{\mathbb{E}\{H_k[n]\}}\right)}\right)\right\} \\ &= \log_2\left(1 + \frac{(1 - \rho_k[n]) p_k[n]}{(1 - \rho_k[n]) \left(\sum_{i \neq k}^K p_i[n] + \frac{\sigma^2}{\xi_k[n]}\right)}\right) \triangleq \tilde{R}_k[n]. \end{aligned} \quad (26)$$

Therefore, the objective function of problem $\mathcal{P}1$ is transformed into \tilde{R}_{sum} , which can be expressed as

$$\tilde{R}_{\text{sum}} = \sum_{n=1}^N \sum_{k=1}^K \tilde{R}_k[n]. \quad (27)$$

B. Optimization of UAV trajectory \mathbf{Q}

For given UAV transmission power allocation \mathbf{p} , user PS ratio $\boldsymbol{\rho}$ and IRS reflection coefficient $\boldsymbol{\theta}$, the UAV trajectory \mathbf{Q} optimization problem can be expressed as

$$\mathcal{P}2: \quad \max_{\mathbf{Q}} \tilde{R}_{\text{sum}}, \quad (28a)$$

$$s.t. \quad (23b), (23c), (23d), (23i). \quad (28b)$$

The problem $\mathcal{P}2$ is still a non-convex optimization problem due to the non-concave objective function and non-convex constraint (28e). Herein, we introduce some auxiliary variables to deal with the problem $\mathcal{P}2$. Let $\{u_k[n] > 0, \forall k, \forall n\}$ denote the upper bound of $\|\mathbf{q}[n] - \mathbf{w}_k\|$, and $\{u[n] > 0, \forall n\}$ denote the upper bound of $\|\mathbf{q}[n] - \mathbf{w}_r\|$. Therefore, they satisfy

$$(u_k[n])^2 \geq \|\mathbf{q}[n] - \mathbf{w}_k\|^2, \forall k, \forall n, \quad (29)$$

and

$$(u[n])^2 \geq \|\mathbf{q}[n] - \mathbf{w}_r\|^2, \forall k. \quad (30)$$

Therefore, the lower bound of the expected combined channel gain, denoted by $\{\underline{\xi}_k[n], \forall k, \forall n\}$, can be expressed as

$$\underline{\xi}_k[n] = \beta_0(u_k[n])^{-\alpha} + \tau_k(u[n])^{-2} + A_k[n], \quad (31)$$

where $\tau_k = \frac{N\beta_0(\beta_0 - \vartheta)}{\|\mathbf{w}_r - \mathbf{w}_k\|^\vartheta}$ and $A_k[n] = \left| \widehat{\mathbf{h}}_{\text{IU},k}^H \Theta[n] \mathbf{h}_{\text{UI}}[n] \right|^2$. In addition, we further introduce the auxiliary variable $\{B_k[n], \forall k, \forall n\}$, which can be given by

$$B_k[n] = \sum_{i \neq k}^K p_i[n] + \frac{\sigma^2}{\underline{\xi}_k[n]}, \quad (32)$$

Accordingly, the objective function of problem $\mathcal{P}2$ can be lower bounded by

$$\tilde{R}_k[n] \geq \log_2 \left(1 + \frac{p_k[n]}{B_k[n]} \right). \quad (33)$$

Therefore, the problem $\mathcal{P}2$ can be equivalently transformed into

$$\mathcal{P}2.1: \quad \max_{\mathbf{Q}, \Upsilon} \sum_{n=1}^N \sum_{k=1}^K \log_2 \left(1 + \frac{p_k[n]}{B_k[n]} \right), \quad (34a)$$

$$\text{s.t.} \quad \underline{\xi}_k[n] \leq \beta_0(u_k[n])^{-\alpha} + \tau_k(u[n])^{-2} + A_k[n], \quad (34b)$$

$$B_k[n] \geq \sum_{i \neq k}^K p_i[n] + \frac{\sigma^2}{\underline{\xi}_k[n]}, \quad (34c)$$

$$\sum_{n=1}^N \left(\rho_k[n] \left(\sum_{i=1}^K p_i[n] \underline{\xi}_k[n] \right) \right) \geq \Xi^{-1} \left(\frac{N\chi_k}{\delta} \right), \quad (34d)$$

$$(23b), (23c), (23d), (29), (30), \quad (34e)$$

where $\Xi^{-1}(x) = b_k - \frac{\ln(\underline{\xi}_k / ((x + Y_k) X_k - 1))}{a_k}$ and $\Upsilon = \{u_k[n], u[n], \underline{\xi}_k[n], B_k[n], \forall k, \forall n\}$ denotes the set of all auxiliary variables. It is worth noting that the problem $\mathcal{P}2$ and $\mathcal{P}2.1$ are completely equivalent². However, the problem $\mathcal{P}2.1$ is still non-convex optimization problem due to the non-concave objective function and non-convex constraints (29), (30) and (34b). Next, we apply SCA to iteratively obtain a suboptimal solution to problem $\mathcal{P}2.1$. We define that $f(B_k[n])$ denote the objective function of the problem $\mathcal{P}2.1$, which is convex with respect to (w.r.t) $B_k[n]$. For the r -th iteration of SCA, the lower bound of $f(B_k[n])$ can be given by Eq. (35) on next page, where $B_k[n]^{(r)}$ is value of the r -th iteration. Similarly, we can apply SCA to carry out the first-order Taylor expansion of the left hand side (LHS) convex functions of constraints (29) and (30), and obtain their lower

bounds respectively. Therefore, constraints (29) and (30) can be written as

$$(u_k[n]^{(r)})^2 + 2u_k[n]^{(r)} (u_k[n] - u_k[n]^{(r)}) \geq \|\mathbf{q}[n] - \mathbf{w}_k\|^2, \forall k, \forall n, \quad (36)$$

and

$$(u[n]^{(r)})^2 + 2u[n]^{(r)} (u[n] - u[n]^{(r)}) \geq \|\mathbf{q}[n] - \mathbf{w}_r\|^2, \forall k. \quad (37)$$

In addition, the right hand side (RHS) of constraint (34b) is intractable due to the AoA in $A_k[n]$ depends on the UAV trajectory in the n -th time slot $\mathbf{q}[n]$. Herein, we introduce the following constraint

$$\|\mathbf{q}[n] - \mathbf{q}[n]^{(r)}\|^2 \leq \delta_{\max}^2, \forall n, \quad (38)$$

where $\mathbf{q}[n]^{(r)}$ is the value of the r -th SCA iteration, and δ_{\max} denotes the maximum allowed displacement of UAV. When the value of δ_{\max} is small enough, we can consider that AoA is approximately unchanged after each iteration. Therefore, $A_k[n]$ also remains unchanged. The $(r+1)$ -th iteration is based on the AoA obtained at the r -th iteration. In order to ensure the accuracy of the approximation, according to [15], we require that the ratio of the maximum allowed deployment of the n -th time slot to the minimum height of the UAV should meet $\delta_{\max}/(h_u)_{\min} \leq \varepsilon_{\max}$, i.e., the value of δ_{\max} under the accuracy threshold ε_{\max} can be represented by $\delta_{\max} \leq (h_u)_{\min} \varepsilon_{\max}^3$. Accordingly, the RHS of constraint (34b) only depends on $u_k[n]$ and $u[n]$. We use the following lemma to deal with constraint (34b).

Lemma 2: For given $a_1 > 0$ and $a_2 > 0$, $g(x_1, x_2) = a_1(x_1)^{-\alpha} + a_2(x_2)^{-2}$ is convex jointly w.r.t. $x_1 > 0$ and $x_2 > 0$.

Let $\tilde{g}(u_k[n], u[n]) = \beta_0(u_k[n])^{-\alpha} + \tau_k(u[n])^{-2}$, since $\beta_0 > 0$ and $\tau_k > 0$, $\tilde{g}(u_k[n], u[n])$ is convex jointly w.r.t. $u_k[n]$ and $u[n]$ according to **Lemma 2**. Thus, constraint (34b) is non-convex constraint. We apply SCA to obtain the lower bound of $\tilde{g}(u_k[n], u[n])$, which can be given by

$$\begin{aligned} \tilde{g}(u_k[n], u[n]) &\geq \beta_0 (u_k[n]^{(r)})^{-\alpha} + \tau_k (u[n]^{(r)})^{-2} - \\ &\alpha \beta_0 (u_k[n]^{(r)})^{-\alpha-1} (u_k[n] - u_k[n]^{(r)}) - 2\tau_k (u[n]^{(r)})^{-3} \\ &(u[n] - u[n]^{(r)}) \triangleq \tilde{g}(u_k[n], u[n])^{lb}, \end{aligned} \quad (39)$$

where $u_k[n]^{(r)}$ and $u[n]^{(r)}$ are the value of the r -th iteration. Therefore, constraint (34b) can be transformed into

$$\underline{\xi}_k[n] \leq \tilde{g}(u_k[n], u[n])^{lb}. \quad (40)$$

Accordingly, the problem $\mathcal{P}2.1$ can be transformed into the

²At the solution to the problem $\mathcal{P}2.1$, if any of constraints in (29) and (30) is satisfied with strict inequality, the corresponding $u_k[n]$ or $u[n]$ can be decreased to make constraint (29) and (30) satisfied with equality. Thus, the corresponding $\underline{\xi}_k[n]$ and $B_k[n]$ can be increased or decreased to make constraint (34b) and (34c) satisfied with equality. Therefore, at the optimal solution to problem $\mathcal{P}2.1$, all constraints must be satisfied with equality, i.e., the problem $\mathcal{P}2$ and $\mathcal{P}2.1$ are equivalent.

³It is worth noting that a sufficiently small ε_{\max} will improve the accuracy of the approximation, but it will also increase the computational complexity. Therefore, the choice of a suitable ε_{\max} can well balance the relationship between accuracy and complexity.

$$f(B_k[n]) \geq \sum_{n=1}^N \sum_{k=1}^K \left(\log_2 \left(1 + \frac{p_k[n]}{B_k[n]^{(r)}} \right) - \frac{p_k[n] (B_k[n] - B_k[n]^{(r)})}{B_k[n]^{(r)} (B_k[n]^{(r)} + 1) \ln 2} \right) \triangleq f(B_k[n])^{lb}, \quad (35)$$

$$\log_2 \left(\sum_{i \neq k}^K p_i[n] + \Delta \right) \leq \log_2 \left(\sum_{i \neq k}^K p_i[n]^{(r)} + \Delta \right) + \frac{\sum_{i \neq k}^K (p_i[n] - p_i[n]^{(r)})}{\left(\sum_{i \neq k}^K p_i[n]^{(r)} + \Delta \right) \ln 2} \triangleq \iota^{ub}, \quad (45)$$

problem $\mathcal{P}2.2$, which can be expressed as

$$\mathcal{P}2.2: \quad \max_{\mathbf{Q}, \Upsilon} f(B_k[n])^{lb}, \quad (41a)$$

$$s.t. \quad (23b), (23c), (23d), (34c), (34d), (36), (37), (40). \quad (41b)$$

The problem $\mathcal{P}2.2$ is a standard convex optimization problem, which can be solved by using CVX toolbox [36].

C. Optimization of PS ratio ρ

For given UAV trajectory \mathbf{Q} , UAV transmission power allocation \mathbf{p} , and IRS reflection coefficient $\boldsymbol{\theta}$, the user PS ratio ρ optimization problem can be transformed into a feasibility-check problem, which can be expressed as

$$\mathcal{P}3: \quad \text{find } \rho_k[n], \quad (42a)$$

$$s.t. \quad (23h), \quad (42b)$$

$$\sum_{n=1}^N \left(\rho_k[n] \left(\sum_{i=1}^K p_i[n] \xi_k[n] \right) \right) \geq \Xi^{-1} \left(\frac{N\chi_k}{\delta} \right). \quad (42c)$$

It can be seen that the problem $\mathcal{P}3$ is a standard linear programming problem, which can be solved by using CVX toolbox [36].

D. Optimization of transmission power allocation \mathbf{p}

For given UAV trajectory \mathbf{Q} , user PS ratio ρ , and IRS reflection coefficient $\boldsymbol{\theta}$, the UAV transmission power allocation \mathbf{p} optimization problem can be expressed as

$$\mathcal{P}4: \quad \max_{\mathbf{p}} \tilde{R}_{\text{sum}}, \quad (43a)$$

$$s.t. \quad (23e), (23f), (23i). \quad (43b)$$

The problem $\mathcal{P}4$ is a non-convex optimization problem due to the non-concave objective function. The objective function of the problem $\mathcal{P}4$ can be further expressed as

$$\tilde{R}_k[n] = \log_2 \left(\sum_{k=1}^K p_k[n] + \Delta \right) - \log_2 \left(\sum_{i \neq k}^K p_i[n] + \Delta \right), \quad (44)$$

where $\Delta = \sigma^2/\xi_k[n]$. $\tilde{R}_k[n]$ is non-concave w.r.t. $p_k[n]$ due to it is a form of difference of concave functions. Thus, we apply SCA to deal with the second term on the RHS of Eq. (44) as Eq.(45) at the top of this page, where $p_i[n]^{(r)}$ is value

of the r -th SCA iteration. Accordingly, the problem $\mathcal{P}4$ can be written as

$$\mathcal{P}4.1: \quad \max_{\mathbf{p}} \sum_{n=1}^N \sum_{k=1}^K \left(\log_2 \left(\sum_{i=1}^K p_i[n] + \Delta \right) - \iota^{ub} \right), \quad (46a)$$

$$s.t. \quad \sum_{n=1}^N \left(\rho_k[n] \left(\sum_{i=1}^K p_i[n] \xi_k[n] \right) \right) \geq \Xi^{-1} \left(\frac{N\chi_k}{\delta} \right), \quad (46b)$$

$$(23e), (23f). \quad (46c)$$

The problem $\mathcal{P}4.1$ is a convex optimization problem, which can be solved by CVX toolbox [36].

E. Optimization of IRS reflection coefficient $\boldsymbol{\theta}$

For given UAV trajectory \mathbf{Q} , user PS ratio ρ , and UAV transmission power allocation \mathbf{p} , the IRS reflection coefficient $\boldsymbol{\theta}$ optimization problem can be expressed as

$$\mathcal{P}5: \quad \max_{\boldsymbol{\theta}} \tilde{R}_{\text{sum}}, \quad (47a)$$

$$s.t. \quad (23g), (23i). \quad (47b)$$

The problem $\mathcal{P}5$ is non-convex due to the non-concave objective function and non-convex constraint (23g) and (23i). We introduce auxiliary variables $\mathbf{a}_k^H[n] = \widehat{\mathbf{h}}_{\text{IU},k}^H \text{diag}(\mathbf{h}_{\text{UI}}[n]) \in \mathbb{C}^{1 \times M}$, $\forall k, n$ and $\mathbf{b} = [e^{j\theta_1[n]}, \dots, e^{j\theta_M[n]}]^T \in \mathbb{C}^{M \times 1}$. Thus, the Eq. (25) can be written as follows

$$\xi_k[n] = \varpi_k[n] + |\mathbf{a}_k^H[n] \mathbf{b}|^2, \quad (48)$$

where $\varpi_k[n] = \frac{\beta_0}{\|\mathbf{q}[n] - \mathbf{w}_k\|^\alpha} + \frac{N\beta_0(\beta_0 - \vartheta)}{\|\mathbf{q}[n] - \mathbf{w}_r\|^2 \|\mathbf{w}_r - \mathbf{w}_k\|^\gamma}$. Let $\mathbf{A}_k[n] = \mathbf{a}_k[n] \mathbf{a}_k^H[n] \in \mathbb{C}^{M \times M}$, $\forall k, n$ and $\mathbf{B} = \mathbf{b} \mathbf{b}^H \in \mathbb{C}^{M \times M}$. They satisfy $\text{rank}(\mathbf{A}_k[n]) = 1$ and $\text{rank}(\mathbf{B}) = 1$. Then constraint (48) can be further transformed into

$$\xi_k[n] = \varpi_k[n] + \text{tr}(\mathbf{A}_k[n] \mathbf{B}). \quad (49)$$

We can apply DC programming to transform the non-convex constraint $\text{rank}(\mathbf{B}) = 1$.

Proposition 1: For the positive semi-definite matrix $\mathbf{M} \in \mathbb{C}^{N \times N}$, $\text{tr}(\mathbf{M}) > 0$, the rank-one constraint can be expressed as the difference between two convex functions, i.e.,

$$\text{rank}(\mathbf{M}) = 1 \Leftrightarrow \text{tr}(\mathbf{M}) - \|\mathbf{M}\|_2 = 0, \quad (50)$$

where $\text{tr}(\mathbf{M}) = \sum_{n=1}^N \sigma_n(\mathbf{M})$, $\|\mathbf{M}\|_2 = \sigma_1(\mathbf{M})$ is spectral

norm, and $\sigma_n(\mathbf{M})$ represents the n -th largest singular value of matrix \mathbf{M} .

According to **Proposition 1**, we transform the non-convex rank-one constraint on matrix \mathbf{B} , and then add it as a penalty term to the objective function of problem $\mathcal{P}5$. Therefore, problem $\mathcal{P}5$ can be transformed into

$$\mathcal{P}5.1: \max_{\mathbf{B}} \tilde{R}_{\text{sum}} - \varsigma (\text{tr}(\mathbf{B}) - \|\mathbf{B}\|_2), \quad (51a)$$

$$\text{s.t. } \sum_{n=1}^N \left(\rho_k [n] \left(\sum_{i=1}^K p_i [n] (\varpi_k [n] + \text{tr}(\mathbf{A}_k [n] \mathbf{B})) \right) \right) \geq \Xi^{-1} \left(\frac{N\chi_k}{\delta} \right), \quad (51b)$$

$$\mathbf{B}_{m,m} = 1, \quad (51c)$$

$$\mathbf{B} \succeq 0, \quad (51d)$$

where $\varsigma \gg 0$ denotes the penalty factor related to the rank-one constraint. The problem $\mathcal{P}5.1$ is non-convex due to the non-concave objective function. Next, we apply SCA to solve it. $\tilde{R}_k [n]$ in the objective function of problem $\mathcal{P}5.1$ can be rewritten as

$$\begin{aligned} \tilde{R}_k [n] &= \log_2 \left((\text{tr}(\mathbf{A}_k [n] \mathbf{B}) + \varpi_k [n]) \sum_{i=1}^K p_i [n] + \sigma^2 \right) \\ &\quad - \log_2 \left((\text{tr}(\mathbf{A}_k [n] \mathbf{B}) + \varpi_k [n]) \sum_{i \neq k}^K p_i [n] + \sigma^2 \right) \\ &\triangleq h_1(\mathbf{B}) - h_2(\mathbf{B}). \end{aligned} \quad (52)$$

For the second term on the LHS of Eq. (52), we use SCA to obtain its upper bound, which can be expressed as

$$h_2(\mathbf{B}) \leq h_2(\mathbf{B}^{(r)}) + \text{tr} \left((\nabla_{\mathbf{B}} h_2(\mathbf{B}^{(r)}))^H (\mathbf{B} - \mathbf{B}^{(r)}) \right) \triangleq h_2(\mathbf{B})^{ub}, \quad (53)$$

where $\mathbf{B}^{(r)}$ is the value of the r -th iteration, and

$$\nabla_{\mathbf{B}} h_2(\mathbf{B}^{(r)}) = \frac{\mathbf{A}_k^H [n] \sum_{i \neq k}^K p_i [n]}{\left((\text{tr}(\mathbf{A}_k [n] \mathbf{B}^{(r)}) + \varpi_k [n]) \sum_{i \neq k}^K p_i [n] + \sigma^2 \right) \ln 2}. \quad \text{In}$$

addition, we can also apply SCA to obtain the lower bound of $\|\mathbf{B}\|_2$ as follows

$$\begin{aligned} \|\mathbf{B}\|_2 &\geq \left\| \mathbf{B}^{(r)} \right\|_2 + \text{tr} \left(\mathbf{u}_{\max}(\mathbf{B}^{(r)}) \mathbf{u}_{\max}(\mathbf{B}^{(r)})^H (\mathbf{B} - \mathbf{B}^{(r)}) \right) \\ &\triangleq (\|\mathbf{B}\|_2)^{lb}, \end{aligned} \quad (54)$$

where $\mathbf{u}_{\max}(\mathbf{B}^{(r)})$ denotes the eigenvector corresponding to the largest singular value of the matrix $\mathbf{B}^{(r)}$. Therefore, the non-convex problem $\mathcal{P}5.1$ can be approximately transformed into

$$\mathcal{P}5.2: \max_{\mathbf{B}} \sum_{n=1}^N \sum_{k=1}^K \left(h_1(\mathbf{B}) - h_2(\mathbf{B})^{ub} - \varsigma (\text{tr}(\mathbf{B}) - (\|\mathbf{B}\|_2)^{lb}) \right), \quad (55a)$$

$$\text{s.t. } (51b), (51c), (51d). \quad (55b)$$

It can be seen that the problem $\mathcal{P}5.2$ is a convex optimization problem, which can be solved by using CVX toolbox [36].

Based on the previous sub-sections, the overall optimization algorithm can be summarized as **Algorithm 1**.

Algorithm 1 Joint UAV Trajectory, UAV Transmission Power Allocation, PS Ratio and IRS Reflection Coefficient Optimization Algorithm

- 1: Initialize $\mathbf{Q}^{(0)}$, $\boldsymbol{\rho}^{(0)}$, $\mathbf{p}^{(0)}$ and $\boldsymbol{\theta}^{(0)}$. Let $r = 0$, $\varepsilon = 10^{-3}$.
 - 2: **repeat**
 - 3: Solve the problem $\mathcal{P}2.2$ for given $\boldsymbol{\rho}^{(r)}$, $\mathbf{p}^{(r)}$ and $\boldsymbol{\theta}^{(r)}$, and obtain UAV trajectory $\mathbf{Q}^{(r+1)}$.
 - 4: Solve the problem $\mathcal{P}3$ for given $\mathbf{Q}^{(r)}$, $\mathbf{p}^{(r)}$ and $\boldsymbol{\theta}^{(r)}$, and obtain PS ratio $\rho^{(r+1)}$.
 - 5: Solve the problem $\mathcal{P}4.1$ for given $\mathbf{Q}^{(r)}$, $\boldsymbol{\rho}^{(r)}$ and $\boldsymbol{\theta}^{(r)}$, and obtain UAV transmission power allocation $\mathbf{p}^{(r+1)}$.
 - 6: Solve the problem $\mathcal{P}5.2$ for given $\mathbf{Q}^{(r)}$, $\boldsymbol{\rho}^{(r)}$ and $\mathbf{p}^{(r)}$, and obtain IRS reflection coefficient $\boldsymbol{\theta}^{(r+1)}$.
 - 7: Update $r = r + 1$.
 - 8: **until** The fractional decrease of the objective value is below a threshold ε .
 - 9: **return** UAV trajectory, UAV transmission power allocation, PS ratio and IRS reflection coefficient.
-

F. Computational Complexity and Convergence Analysis

1) *Computational complexity analysis*: In each iteration, the problem $\mathcal{P}2.2$ is solved with the complexity of $\mathcal{O}(N)$, the problem $\mathcal{P}3$ and problem $\mathcal{P}4.1$ both are solved with computational complexity of $\mathcal{O}(KN)$. The problem $\mathcal{P}5.2$ solves a relaxed SDP problem by interior point method, so the computational complexity can be represented by $\mathcal{O}((M+1)^{3.5})$. We assume that the number of iterations required for the algorithm to reach convergence is r , the computational complexity of the proposed algorithm can be expressed as $\mathcal{O}(r(N + KN + (M+1)^{3.5}))$.

2) *Convergence analysis*: The convergence of the proposed joint UAV trajectory, UAV transmission power allocation, PS ratio and IRS reflection coefficient optimization in IRS empowered UAV SWIPT networks can be elaborated as follows.

We define $\mathbf{Q}^{(r)}$, $\boldsymbol{\rho}^{(r)}$, $\mathbf{p}^{(r)}$ and $\boldsymbol{\theta}^{(r)}$ as the r -th iteration solution of the problem $\mathcal{P}2.2$, $\mathcal{P}3$, $\mathcal{P}4.1$ and $\mathcal{P}5.2$. Herein, the objective function is denoted by $\Re(\mathbf{Q}^{(r)}, \boldsymbol{\rho}^{(r)}, \mathbf{p}^{(r)}, \boldsymbol{\theta}^{(r)})$. In the step 3 of **Algorithm 1**, since the UAV trajectory can be obtained for given $\boldsymbol{\rho}^{(r)}$, $\mathbf{p}^{(r)}$ and $\boldsymbol{\theta}^{(r)}$. Hence, we have

$$\Re(\mathbf{Q}^{(r)}, \boldsymbol{\rho}^{(r)}, \mathbf{p}^{(r)}, \boldsymbol{\theta}^{(r)}) \leq \Re(\mathbf{Q}^{(r+1)}, \boldsymbol{\rho}^{(r)}, \mathbf{p}^{(r)}, \boldsymbol{\theta}^{(r)}). \quad (56)$$

Similarly, in the step 4 of **Algorithm 1**, we can obtain the PS ratio when $\mathbf{Q}^{(r+1)}$, $\mathbf{p}^{(r)}$ and $\boldsymbol{\theta}^{(r)}$ are given. Herein, we also have

$$\Re(\mathbf{Q}^{(r+1)}, \boldsymbol{\rho}^{(r)}, \mathbf{p}^{(r)}, \boldsymbol{\theta}^{(r)}) \leq \Re(\mathbf{Q}^{(r+1)}, \boldsymbol{\rho}^{(r+1)}, \mathbf{p}^{(r)}, \boldsymbol{\theta}^{(r)}). \quad (57)$$

In the step 5 of **Algorithm 1**, UAV transmission power allocation can be obtained when $\mathbf{Q}^{(r+1)}$, $\boldsymbol{\rho}^{(r+1)}$ and $\boldsymbol{\theta}^{(r)}$ are given. Therefore, we have

$$\Re(\mathbf{Q}^{(r+1)}, \boldsymbol{\rho}^{(r+1)}, \mathbf{p}^{(r)}, \boldsymbol{\theta}^{(r)}) \leq \Re(\mathbf{Q}^{(r+1)}, \boldsymbol{\rho}^{(r+1)}, \mathbf{p}^{(r+1)}, \boldsymbol{\theta}^{(r)}). \quad (58)$$

Finally, in the step 6 of **Algorithm 1**, IRS reflection coefficient can be obtained when $\mathbf{Q}^{(r+1)}$, $\boldsymbol{\rho}^{(r+1)}$ and $\mathbf{p}^{(r+1)}$ are fixed.

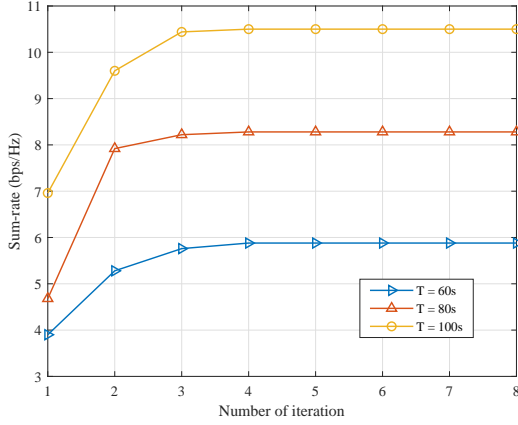


Fig. 3. Convergence behaviour of the proposed optimization algorithm.

Therefore, we have

$$\Re(\mathbf{Q}^{(r+1)}, \boldsymbol{\rho}^{(r+1)}, \mathbf{p}^{(r+1)}, \boldsymbol{\theta}^{(r)}) \leq \Re(\mathbf{Q}^{(r+1)}, \boldsymbol{\rho}^{(r+1)}, \mathbf{p}^{(r+1)}, \boldsymbol{\theta}^{(r+1)}). \quad (59)$$

Based on the above, we can obtain

$$\Re(\mathbf{Q}^{(r)}, \boldsymbol{\rho}^{(r)}, \mathbf{p}^{(r)}, \boldsymbol{\theta}^{(r)}) \leq \Re(\mathbf{Q}^{(r+1)}, \boldsymbol{\rho}^{(r+1)}, \mathbf{p}^{(r+1)}, \boldsymbol{\theta}^{(r+1)}), \quad (60)$$

which shows that the value of the objective function is non-decreasing after each iteration of **Algorithm 1**. Since the objective function values of problems $\mathcal{P}2.2$, $\mathcal{P}3$, $\mathcal{P}4.1$ and $\mathcal{P}5.2$ have a finite upper bound, the convergence of **Algorithm 1** can be guaranteed.

IV. NUMERICAL SIMULATION

In this section, we verify the effectiveness of the proposed algorithm through numerical simulation. In this paper, we consider that $K = 6$ ground users are randomly distributed in a 500×500 circular area. We assume that the UAV flies at a fixed height $h_u = 100\text{m}$, and its maximum flight speed $V_{max} = 20\text{m/s}$. The maximum transmit power of UAV is $P_{max} = 43\text{dBm}$. The coordinates of the initial horizontal position and final horizontal position of the UAV are $(0, 250)$ and $(500, 250)$, respectively. In addition, we consider that the IRS is fixed on a building with a height of $h_r = 30\text{m}$, and its horizontal position coordinate is $(250, 0)$. The number of IRS reflecting elements is $M = 20$. The channel power gain at when the reference distance $d_0 = 1\text{m}$ is $\beta_0 = -30\text{dB}$. We assume that the parameters of all users are the same, i.e., $\xi_k = 24\text{mW}$, $a_k = 150$ and $b_k = 0.024$ [37]. The Rice factor is $\kappa = 3\text{dB}$. The additive white Gaussian noise of the transmission channel is $\sigma = -80\text{dBm}$. The threshold of proposed algorithm is set as 10^{-3} .

We first evaluate the convergence of the proposed algorithm. Fig. 3 shows the change of sum-rate with the number of iteration under different time periods T . We can see that the sum-rate increases rapidly with the number of iteration and can reach stable convergence in about 4 iterations, which verifies the convergence of the proposed algorithm.

Next, we elaborate the optimized trajectory of UAV at different time periods T assisted by IRS formed by the proposed

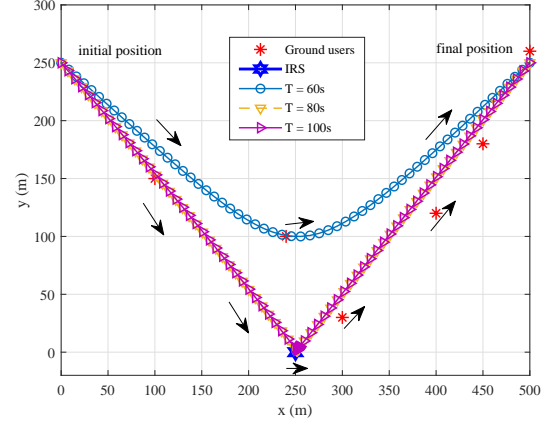


Fig. 4. UAV optimization trajectory at different time periods T assisted by IRS.

algorithm in Fig. 4. From Fig. 4, we can see that when the time period T is larger, UAV can be closer to more ground users, providing better wireless information transmission and wireless energy transmission. With the assistance of IRS, UAV can fly to IRS to balance the channel conditions of UU-link and combined channels to provide better quality-of-service (QoS) for ground users. In addition, when the time period T is large enough, the UAV spends more time staying near the IRS to provide higher quality services for ground users.

In Fig. 5, we compare the change of sum-rate with the UAV height h_u under different IRS reflecting elements. With the assistance of IRS, our proposed algorithm has a more obvious gain in terms of sum-rate compared to the scheme without IRS assistance. The assistance of IRS is equivalent to an additional set of adjustable combined channels, which can better improve the system performance. In addition, the number of IRS reflecting elements also has an effect on the sum-rate. Specifically, as the number of IRS reflecting elements increases, the sum-rate will increase accordingly. This is because as the number of IRS reflecting elements increases, the number of combined channels will also increase, which can provide better channel quality for ground users, i.e., the sum-rate will also increase accordingly. When the number of IRS reflecting elements is fixed, the lower the UAV's flight height, the greater sum-rate. This is mainly because when the UAV is close to the ground user, the quality of the air-ground channel provided can be improved, thus the user's rate can also be increased.

Then, we compare the proposed algorithm with several other algorithms as follows: (1) Ran-static: Random deployment of static UAV. (2) Opt-static: Optimized deployment of static UAV. (3) Equ-power: UAV with equal transmit power. (4) Non-max-rate: UAV without maximum flight rate constraint. (5) Str-trajectory: UAV flies in a straight line from the initial position to the final position. For Ran-static and Opt-static, the optimization of other variables is the same as the proposed algorithm except that UAV trajectory optimization is not considered. They consider the static deployment problem of UAV. Ran-static considers the UAV to be deployed at

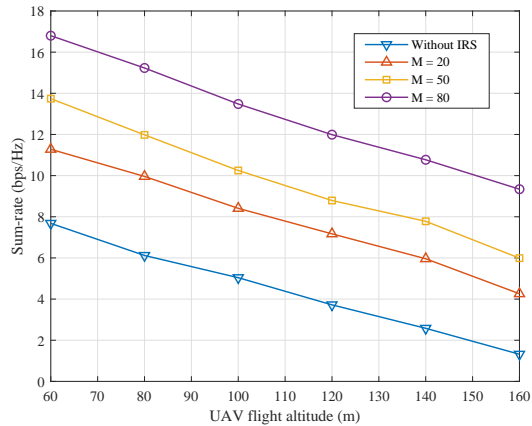


Fig. 5. Sum-rate versus the UAV flight altitude with different IRS reflecting elements.

a random position in the circular area, and Opt-static uses the Exhaustive method to find the sub-optimal deployment position of the circular area after optimizing other variables at a certain step. Hence, compared with Ran-static, Opt-static has better performance in terms of sum-rate. However, the proposed algorithm considers the UAV's optimized trajectory. The UAV can fly dynamically and serve as many ground users as possible. Therefore, the performance of the algorithm has a significant gain compared to Ran-static and Opt-static. Equ-power considers the equal distribution of UAV power, i.e., for all users to distribute the same power, the rate of users farther from UAV will be reduced. Therefore, the proposed algorithm considering UAV power optimization has a gain in terms of sum-rate compared to Equ-power. Next, we consider the case that the UAV without maximum flight rate constraint, i.e., Non-max-rate. In Non-max-rate, the UAV can hover directly above each ground user long enough without considering the flight rate constraints, and then fly to the next user, which can significantly improve the throughput of ground users. Therefore, compared with the proposed algorithm, the performance of this algorithm in terms of sum-rate is better. However, in practical scenarios, UAV usually has a maximum flight rate constraint. In summary, the proposed algorithm is closer to the practical setup and has a higher performance gain compared to several algorithms.

Fig. 6 shows the effect of UAV on system performance with dynamic flight and static deployment. Next, Fig. 7 illustrates the effect of different UAV trajectory schemes in terms of sum-rate. Non-max-rate has been mentioned above, here we can understand it as a UAV trajectory scheme, that is, UAV provides services to ground users through hover-flight. UAV flies directly above each user to provide services, and then flies to another user. Therefore, compared to the proposed algorithm, the rate of each user can be improved. In Str-trajectory, UAV does not fly according to the user's position, and not all users' rates are guaranteed, so sum-rate will decrease compared to the proposed algorithm.

In Fig. 8, the sum-rate versus UAV maximum transmission power with different time periods T is shown. It can be seen

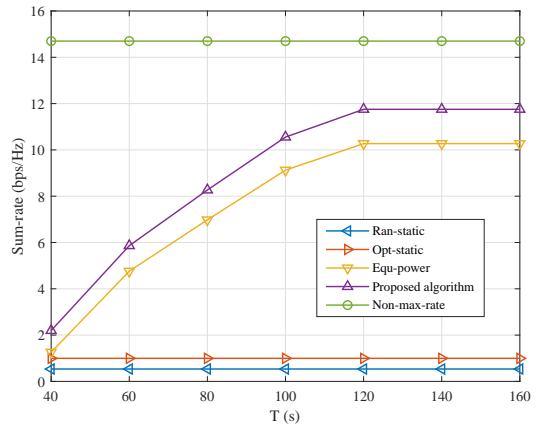


Fig. 6. Sum-rate versus time period T for the proposed algorithm and other algorithms.

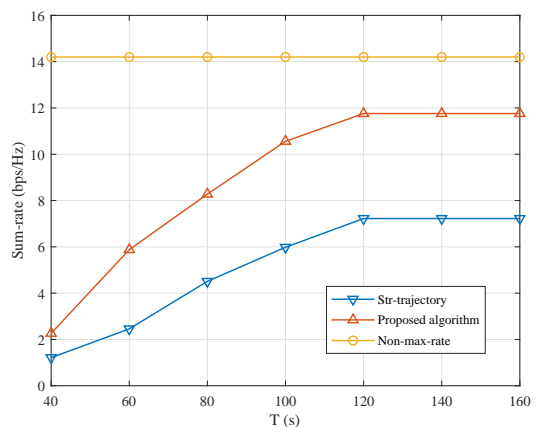


Fig. 7. Sum-rate versus time period T with different UAV trajectory designs.

that when the UAV maximum transmission power is fixed, the sum-rate increases with the increase of the time period T . This is mainly due to the increase in maximum transmission power during time period T , UAV can transmit a stronger signal, improving users' rate. In addition, when the UAV maximum transmission power increases, the sum-rate will also increase, which can be explained as the increase of the UAV transmit power, the rate of all users can be improved, so sum-rate of system will also increase.

Finally, in Fig. 9, we describe the change of sum-rate with the ground user energy threshold under different UAV maximum flight speed. It can be seen from Fig. 9 that when the energy threshold of ground user is fixed, the maximum flight speed of UAV has a relatively large impact on the sum-rate, i.e., the sum-rate increases as the UAV maximum flight rate increases. This is because the greater the UAV maximum flight speed, the longer UAV can hover at the user, so it can provide better service for ground users. In addition, considering the SWIPT system in this paper, the change of sum-rate with the energy threshold of ground users reflects the trade-off of the SWIPT system. When the energy threshold of ground user continues to increase, i.e., the user's energy requirement be-

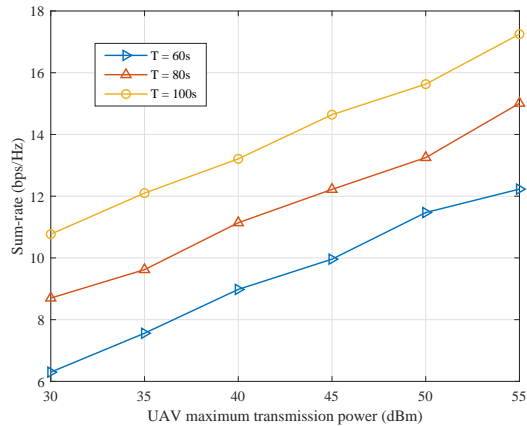


Fig. 8. Sum-rate versus UAV maximum transmission power with different time periods T .

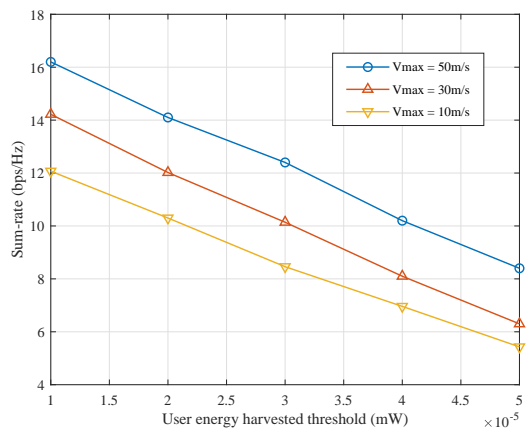


Fig. 9. Sum-rate versus user energy harvested threshold with different UAV maximum flight speed.

comes greater, the sum-rate of system will gradually decrease. The main reason is that the increase in energy requirements of ground users triggers the power splitting ratio to use more power resources of UAV for wireless energy transmission and a smaller portion for wireless information transmission, which leads to a reduction in the rate of ground users.

V. CONCLUSION

This paper investigates the sum-rate maximization problem of IRS empowered UAV SWIPT networks. Specifically, under the constraints of the energy harvested threshold, UAV trajectory, UAV transmission power allocation, PS ratio and IRS reflection coefficient are jointly optimized. First, we transform the problem. Then, in order to solve the transformed problem, we apply the AO algorithm framework which is divided into four blocks for solving. Specifically, when the other three variables are given, we apply SCA and DC programming to alternately optimize the four optimization variables until convergence is achieved. Then, the computational complexity and convergence analysis of the proposed algorithm is given. Finally, the numerical simulation results verify the convergence and effectiveness of the algorithm, which shows that

the proposed algorithm can significantly improve the sum-rate of the system, and the role of IRS is extremely important, and the system performance can be improved at a lower cost, which is very meaningful.

REFERENCES

- [1] D. Xu and H. Zhu, "Secure transmission for SWIPT IoT systems with full-duplex IoT devices," *IEEE Internet Things J.*, vol. 6, no. 6, pp. 10915–10933, 2019.
- [2] G. Bedi, G. K. Venayagamoorthy, R. Singh, R. R. Brooks, and K.-C. Wang, "Review of internet of things (IoT) in electric power and energy systems," *IEEE Internet Things J.*, vol. 5, no. 2, pp. 847–870, 2018.
- [3] H.-T. Ye, X. Kang, J. Joung, and Y.-C. Liang, "Optimization for full-duplex rotary-wing UAV-enabled wireless-powered IoT networks," *IEEE Trans. Wireless Commun.*, vol. 19, no. 7, pp. 5057–5072, 2020.
- [4] I. Budhiraja, N. Kumar, S. Tyagi, S. Tanwar, and M. Guizani, "SWIPT-enabled D2D communication underlying NOMA-based cellular networks in imperfect CSI," *IEEE Trans. Veh. Technol.*, vol. 70, no. 1, pp. 692–699, 2021.
- [5] R. Ma, H. Wu, J. Ou, S. Yang, and Y. Gao, "Power splitting-based SWIPT systems with full-duplex jamming," *IEEE Trans. Veh. Technol.*, vol. 69, no. 9, pp. 9822–9836, 2020.
- [6] A. Li and C. Masouros, "Energy-efficient SWIPT: From fully digital to hybrid analog-digital beamforming," *IEEE Trans. Veh. Technol.*, vol. 67, no. 4, pp. 3390–3405, 2018.
- [7] D. Song, W. Shin, J. Lee, and H. V. Poor, "Sum-throughput maximization in NOMA-based WPCN: A cluster-specific beamforming approach," *IEEE Internet Things J.*, pp. 1–1, 2021.
- [8] L. Xie, J. Xu, and R. Zhang, "Throughput maximization for UAV-enabled wireless powered communication networks," *IEEE Internet Things J.*, vol. 6, no. 2, pp. 1690–1703, 2019.
- [9] Q. Shi, L. Liu, W. Xu, and R. Zhang, "Joint transmit beamforming and receive power splitting for MISO SWIPT systems," *IEEE Trans. Wireless Commun.*, vol. 13, no. 6, pp. 3269–3280, 2014.
- [10] S. Zhang, H. Zhang, B. Di, and L. Song, "Cellular UAV-to-x communications: Design and optimization for multi-UAV networks," *IEEE Trans. Wireless Commun.*, vol. 18, no. 2, pp. 1346–1359, 2019.
- [11] Z. Li, Y. Wang, M. Liu, R. Sun, Y. Chen, J. Yuan, and J. Li, "Energy efficient resource allocation for UAV-assisted space-air-ground Internet of remote things networks," *IEEE Access*, vol. 7, pp. 145 348–145 362, 2019.
- [12] P. S. Bithas, V. Nikolaidis, A. G. Kanatas, and G. K. Karagiannidis, "UAV-to-ground communications: Channel modeling and UAV selection," *IEEE Trans. Commun.*, vol. 68, no. 8, pp. 5135–5144, 2020.
- [13] Y. Zeng and R. Zhang, "Energy-efficient UAV communication with trajectory optimization," *IEEE Trans. Wireless Commun.*, vol. 16, no. 6, pp. 3747–3760, 2017.
- [14] Y. Cai, F. Cui, Q. Shi, M. Zhao, and G. Y. Li, "Dual-UAV-enabled secure communications: Joint trajectory design and user scheduling," *IEEE J. Sel. Areas Commun.*, vol. 36, no. 9, pp. 1972–1985, 2018.
- [15] Q. Wu, Y. Zeng, and R. Zhang, "Joint trajectory and communication design for multi-UAV enabled wireless networks," *IEEE Trans. Wireless Commun.*, vol. 17, no. 3, pp. 2109–2121, 2018.
- [16] Y. Wang, Z. Li, Y. Chen, M. Liu, X. Lyu, X. Hou, and J. Wang, "Joint resource allocation and UAV trajectory optimization for space-air-ground Internet of remote things networks," *IEEE Syst. J.*, pp. 1–11, 2020.
- [17] X. Sun, W. Yang, Y. Cai, and M. Wang, "Secure mmwave UAV-enabled SWIPT networks based on random frequency diverse arrays," *IEEE Internet Things J.*, vol. 8, no. 1, pp. 528–540, 2021.
- [18] X. Sun, W. Yang, and Y. Cai, "Secure communication in NOMA-assisted millimeter-wave SWIPT UAV networks," *IEEE Internet Things J.*, vol. 7, no. 3, pp. 1884–1897, 2020.
- [19] W. Wang, J. Tang, N. Zhao, X. Liu, X. Y. Zhang, Y. Chen, and Y. Qian, "Joint precoding optimization for secure SWIPT in UAV-aided NOMA networks," *IEEE Trans. Commun.*, vol. 68, no. 8, pp. 5028–5040, 2020.
- [20] S. Yin, Y. Zhao, L. Li, and F. R. Yu, "UAV-assisted cooperative communications with power-splitting information and power transfer," *IEEE Trans. Green Commun. and Networking*, vol. 3, no. 4, pp. 1044–1057, 2019.
- [21] Z. Chen, K. Chi, K. Zheng, G. Dai, and Q. Shao, "Minimization of transmission completion time in UAV-enabled wireless powered communication networks," *IEEE Internet Things J.*, vol. 7, no. 2, pp. 1245–1259, 2020.

- [22] L. Xie, J. Xu, and Y. Zeng, "Common throughput maximization for UAV-enabled interference channel with wireless powered communications," *IEEE Trans. Commun.*, vol. 68, no. 5, pp. 3197–3212, 2020.
- [23] Q. Wu and R. Zhang, "Intelligent reflecting surface enhanced wireless network via joint active and passive beamforming," *IEEE Trans. Wireless Commun.*, vol. 18, no. 11, pp. 5394–5409, 2019.
- [24] Q. Wu and R. Zhang, "Beamforming optimization for wireless network aided by intelligent reflecting surface with discrete phase shifts," *IEEE Trans. Commun.*, vol. 68, no. 3, pp. 1838–1851, 2020.
- [25] Q. Wu and R. Zhang, "Joint active and passive beamforming optimization for intelligent reflecting surface assisted SWIPT under QoS constraints," *IEEE J. Sel. Areas Commun.*, vol. 38, no. 8, pp. 1735–1748, 2020.
- [26] M.-M. Zhao, A. Liu, Y. Wan, and R. Zhang, "Two-timescale beamforming optimization for intelligent reflecting surface aided multiuser communication with QoS constraints," *IEEE Trans. Wireless Commun.*, pp. 1–1, 2021.
- [27] S. Gong, X. Lu, D. T. Hoang, D. Niyato, L. Shu, D. I. Kim, and Y.-C. Liang, "Towards smart radio environment for wireless communications via intelligent reflecting surfaces: A comprehensive survey," *arXiv preprint arXiv:1912.07794*, 2019.
- [28] W. Tang, M. Z. Chen, X. Chen, J. Y. Dai, Y. Han, M. Di Renzo, Y. Zeng, S. Jin, Q. Cheng, and T. J. Cui, "Wireless communications with reconfigurable intelligent surface: Path loss modeling and experimental measurement," *IEEE Trans. Wireless Commun.*, vol. 20, no. 1, pp. 421–439, 2021.
- [29] T. Shafique, H. Tabassum, and E. Hossain, "Optimization of wireless relaying with flexible UAV-borne reflecting surfaces," *IEEE Trans. Commun.*, vol. 69, no. 1, pp. 309–325, 2021.
- [30] Z. Wei, Y. Cai, Z. Sun, D. W. K. Ng, J. Yuan, M. Zhou, and L. Sun, "Sum-rate maximization for IRS-assisted UAV OFDMA communication systems," *IEEE Trans. Wireless Commun.*, vol. 20, no. 4, pp. 2530–2550, 2021.
- [31] S. Fang, G. Chen, and Y. Li, "Joint optimization for secure intelligent reflecting surface assisted UAV networks," *IEEE Wireless Commun. Lett.*, vol. 10, no. 2, pp. 276–280, 2021.
- [32] X. Mu, Y. Liu, L. Guo, J. Lin, and H. V. Poor, "Intelligent reflecting surface enhanced multi-UAV NOMA networks," *arXiv preprint arXiv:2101.09145*, 2021.
- [33] S. Li, B. Duo, M. Di Renzo, M. Tao, and X. Yuan, "Robust secure UAV communications with the aid of reconfigurable intelligent surfaces," *IEEE Trans. Wireless Commun.*, pp. 1–1, 2021.
- [34] K. Xiong, B. Wang, and K. J. R. Liu, "Rate-energy region of SWIPT for MIMO broadcasting under nonlinear energy harvesting model," *IEEE Trans. Wireless Commun.*, vol. 16, no. 8, pp. 5147–5161, 2017.
- [35] M. Hua, L. Yang, Q. Wu, and A. L. Swindlehurst, "3D UAV trajectory and communication design for simultaneous uplink and downlink transmission," *IEEE Trans. Commun.*, vol. 68, no. 9, pp. 5908–5923, 2020.
- [36] M. Grant and S. Boyd, "CVX: Matlab software for disciplined convex programming, version 2.1," 2014.
- [37] Y. Lu, K. Xiong, P. Fan, Z. Ding, Z. Zhong, and K. B. Letaief, "Global energy efficiency in secure MISO SWIPT systems with nonlinear power-splitting EH model," *IEEE J. Sel. Areas Commun.*, vol. 37, no. 1, pp. 216–232, 2019.